Molecular Medicine

Pigment Epithelium-Derived Factor (PEDF) Peptide Eye Drops Reduce Inflammation, Cell Death and Vascular Leakage in Diabetic Retinopathy in *Ins2*^{Akita} Mice

Yanling Liu,[1] Lan Franco Leo,[1] Corban McGregor,[1] Anzor Grivitishvili,[1] Colin J Barnstable,[1] and Joyce Tombran-Tink[1,2]

[1]Department of Neural and Behavioral Sciences and [2]Department of Ophthalmology, Pennsylvania State University College of Medicine, Hershey, Pennsylvania, United States of America

Inflammation, neurodegeneration and microvascular irregularities are included in the spectrum of defects associated with diabetic retinopathy. Here, we evaluated intraocular deliverability features of two pigment epithelium-derived factor (PEDF) derivatives given as eye drops and their efficacy in modulating diabetes-induced retinal complications. The antiangiogenic PEDF60–77 (P60) and neuroprotective PEDF78–121 (P78) derivatives were applied to *Ins2*^{Akita} mouse eyes once a week for 15 wks at the onset of hyperglycemia. Peptides, labeled with Alexa Fluor 488, were observed penetrating the cornea by 1–4 h and gained access to the ciliary body, retinal pigment epithelium (RPE)-choroid complex, retina microvasculature and vitreous. Peak vitreous levels were 0.2 μg/mL for P60 and 0.9 μg/mL for P78 after 0.5 and 4 h, respectively. Both peptides reduced vascular leakage by ~60% and increased zona occludens 1 (ZO1) and occludin expression in the microvasculature to nondiabetic levels. P60 induced pERK1/2 and P78 promoted pAKT in Muller glia, two signals that were dampened in diabetic conditions. Pharmacologically inhibiting AKT signaling in the retina blocked effects of the peptides on ZO1 and occludin expression. P78 reduced levels of 9/20 cytokines in diabetic vitreous including interferon (IFN)-γ, interleukin (IL)-6, IL-3 and tumor necrosis factor (TNF)-α. P60 lowered levels of 6/20 cytokines but was less effective than P78. Neuroprotective P78 prevented diabetes-induced microglia activation by ~60%, retinal ganglion cell (RGC) death by ~22% and inner plexiform layer thinning by ~13%. In summary, we provide evidence that PEDF bioactive derivatives gained access to the retina by topical delivery and validated their efficacy in reducing diabetic retinopathy complications. Our findings argue for glia regulation of microvascular leakage and an early root cause for RGC degeneration embedded in microglia activation.

Online address: http://www.molmed.org
doi: 10.2119/molmed.2012.00008

INTRODUCTION

Diabetes can cause damage to the retina that results in severe loss of vision. Despite advances in medical care, therapeutic options for patients are inadequate because of the complex etiology of this disease. The January 2011 National Diabetes Fact Sheet reports that 25.8 million (8.3%) Americans have diabetes and ~12% of these will develop retinopathy, with severity dependent on the duration of diabetes and extent of glycemic control.

Vision is compromised during the late stages of diabetic retinopathy primarily because of vascular complications and macular edema (1–4), but events that initiate such damage are believed to occur earlier (5). Given the alarming prevalence of diabetes, less invasive and cost-effective therapeutics for diabetic retinopathy are necessary.

Some of the most visible ophthalmoscopic signs in the diabetic retina are vascular lesions, which include microaneurysms, capillary degeneration, vessel growth in the normally avascular vitreous, increased vascular permeability and hemorrhaging. These features have led to the initial belief that diabetic retinopathy is exclusively a disease of the microvasculature, an assumption that is rapidly changing as recent findings challenge old ideas and give new insights into the complexities of diabetic retinopathy. These include the less visible signs of neuronal cell death, alterations in glia cell structure and function, and inflammation (6).

Diabetic complications are fueled by impairment of specific central nervous system circuits, metabolism, insulin production and function and other actions that alter glucose homeostasis (7,8). Deci-

Address correspondence to *Joyce Tombran-Tink, Penn State University College of Medicine, 500 University Drive, Hershey, PA 17033. Phone: 717-531-7475; Fax: 717-531-5184; E-mail: jttink@aol.com.*
Submitted January 9, 2012; Accepted for publication September 20, 2012; Epub (www.molmed.org) ahead of print September 20, 2012.

The Feinstein Institute for Medical Research North Shore LIJ

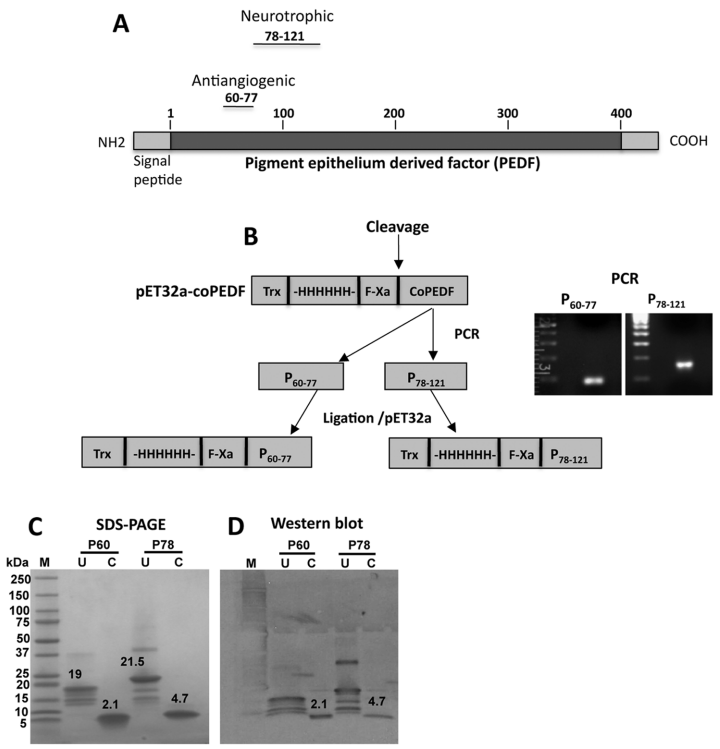

Figure 1. Expression and purification of the antiangiogenic (P60) and neuroprotective (P78) PEDF derivatives. (A) The N-terminal locations of P60 at residues 60–77 and P78 at residues 78–121 of the PEDF protein are indicated in the diagram. (B) Schematic showing cloning of the peptide derivatives into pET32a. Bands on the PCR gels represent the amplified P60 and P78 fragments. (C) On the SDS-PAGE gradient gel (4–20%) expression of P60 and P78 (U, uncleaved from the upstream thioredoxin vector sequence) and purity of the peptides after cleavage (C, cleaved) at 2.1 and 4.7 kDa, respectively, are shown (M, Bio-Rad Precision Plus Protein™ Dual Xtra Standards). (D) The Western blot confirms identity of the two fragments by using a PEDF polyclonal antibody. Calculated yields of the expressed (U) and purified (C) peptides are given in Table 1.

phering how these disturbances translate into damage to the retina is still a work in progress. Key suspects in the progression of the disease include vascular endothelial growth factor (VEGF) and extracellular carbonic anhydrase (8–10), insulin like growth factor (11), pigment epithelium-derived factor (PEDF) (12–14), occludin and claudin (6,15,16), protein kinase C (17), erythropoietin (18), advanced glycation end products (19) and inflammatory cytokines (20). Recent work suggests that retinal neurons, pericytes, glia and endothelial cells are all affected in diabetic retinopathy (6,21). This list emphasizes the multiple effects of diabetes on the retina and the need for combinatorial treatment approaches.

It is clear that diabetes triggers a range of structural changes in the retina but what is not apparent is the relationship between these events and when they occur during disease progression. This result presents an obstacle to developing treatments. As of yet, there are no clinically approved therapies for diabetic retinopathy. In this study, we examined whether small neuroprotective and antiangiogenic fragments of PEDF (22–24) have access to the retina in doses that can reduce retinopathy when administered as eye drops in a mouse model of diabetes (4). PEDF is a large 50-kDa polypeptide that is native to the eye and has dual effects in reducing pathologies in the retina. It blocks neovascularization when injected intravitreally as a bolus or by using viral-mediated strategies (22–24). A second feature of PEDF is its known neuroprotective actions on photoreceptors and retinal ganglion cells in models of retinal degeneration. We and others have identified the PEDF neuroprotective and antiangiogenic activities on two short adjacent N-terminal fragments of the gene (24–27). In this study, we examined the deliverability of these PEDF derivatives to the retina in eye drops; examined their utility in reducing inflammation, neurodegeneration and microvascular dysfunction in the diabetic retina; and exploited their activity to dissect possible root mechanisms in the development of the disease.

Table 1. Peptide yield.

	mg/L	mg/g cells
Uncleaved P60	73.9	33.5
Cleaved P60	14.8	6.8
Uncleaved P78	76.4	34.7
Cleaved P78	17.1	7.8

MATERIALS AND METHODS

We used pET32a vector, Ni-NTA His•Bind Purification resin, and enterokinase (Novagen; EMD Millipore, Billerica, MA, USA). Factor Xa was obtained from New England Biolabs (Beverly, MA, USA); and ketamine and xylazine were obtained from Phoenix Pharmaceutical (St. Joseph, MO, USA) and LLOYD Laboratories (Shenandoah, IA, USA), respectively. Fluorescein isothiocyanate (FITC)-labeled bovine serum albumin (BSA) (BSA-FITC) was obtained from Sigma (St. Louis, MO, USA). The occludin polyclonal antibody (pAb), Alexa Fluor 488 and BL21Star(DE3) immunocompetent cells were all obtained from Cell Signaling (Danvers, MA, USA); pAkt (pAb), the monoclonal antibodies (mAbs) for pERK1/2, and glial fibrillary acidic protein (GFAP) from Santa Cruz Biotechnology (Santa Cruz, CA, USA); ionized calcium-binding adaptor molecule 1 (IBA1) pAb from Wako (Richmond, VA, USA); actin mAbs

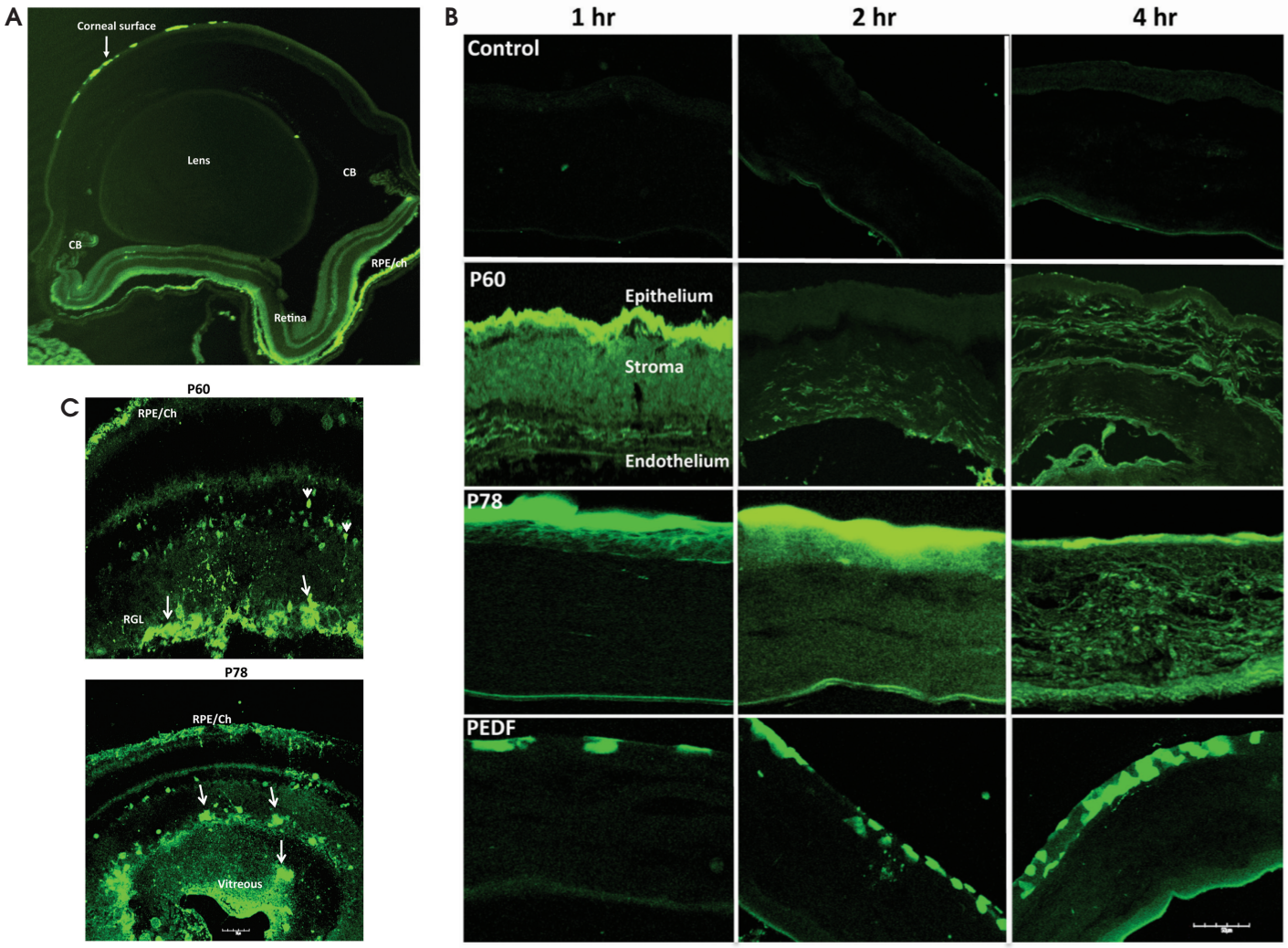

Figure 2. Penetration of topically applied Alexa Fluor 488–labeled P60 (5 μg) and P78 in ATs across a diabetic (>300 mg/dL glucose) *Ins2*^{Akita} mouse eye. (A) Cross-section of a mouse eye 2 h after receiving the eye drops. The fluorescently labeled peptides were visible on the corneal surface and in the ciliary body (CB), RPE/Choroid (RPE/ch) and retina (n = 8). (B) Cross-sections of the corneal epithelium 1–4 h after treatment with eye drops containing dialyzed unconjugated Alexa Fluor 488 label (control), labeled P60, P78 or PEDF. Controls receiving dialyzed unconjugated Alexa Fluor 488 alone indicate that most of the free label was removed during dialysis. Labeled P60 penetrated the cornea earlier than P78, and most of the larger full-length PEDF (50 kDa) remained at the corneal epithelium (n = 5) (scale bar = 50 μmol/L). (C) Distribution of labeled P60 and P78 in the retina, 2 h after eye drops were given. The fluorescently labeled peptides were visible in the RPE/choroid, vitreous and vasculature of the inner retina (arrows) and in some retinal cells (arrowheads). RPE/Ch: RPE-choroidal complex (n = 4) (scale bar = 50 μmol/L).

from EMD Millipore; and albumin pAb from Epitomics (Burlingame, CA, USA). The Cy3 conjugated immunoglobulin G (IgG) secondary antibodies: goat anti-mouse and goat anti-rabbit IgG were obtained from Jackson ImmunoResearch (West Grove, PA, USA). The pharmacological inhibitors of phosphatidylinositol 3-kinase (PI3K) (iPI3K; LY294,002) and the mitogen-activated protein (MAP) kinase (iMAPK; U0126) pathways and zona occludens 1 (ZO1) pAbs were obtained from Cell Signaling. Chemiluminescent reagents were purchased from Thermo Scientific (Rockford, IL, USA), Kodak Scientific Imaging X-OMAT LS Film from Carestream Health (Rochester, NY, USA), Dulbecco's modified Eagle medium (DMEM) from Life Technologies (GIBCO; Carlsbad, CA, USA) and the Affymetrix Procarta mouse cytokine profiling platforms from Panomics (Fremont, CA, USA). RNeasy and Taq polymerase chain reaction (PCR) master mix were obtained from Qiagen (Valencia, CA, USA), Superscript First Strand Synthesis System from Life Technologies (Invitrogen) and iQ SYBR Green Supermix solution from Bio-Rad (Hercules, CA, USA).

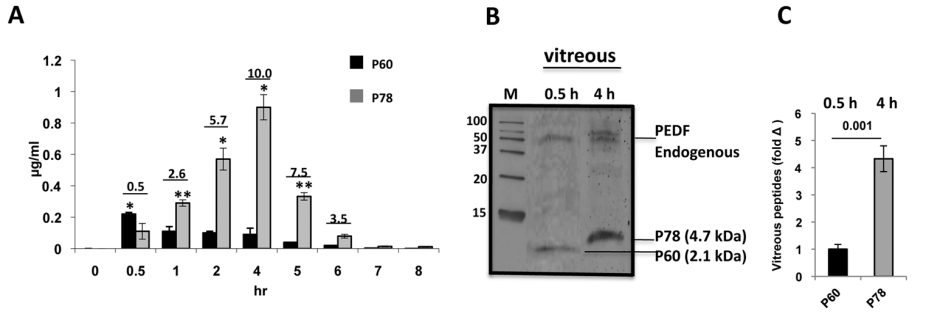

Figure 3. Detection of Alexa Fluor 488–labeled P60 and P78 in rat vitreous after corneal application. (A) Fluorimetric detection of peptide levels in the vitreous. Peak levels of 0.2 ng/mL for P60 and 0.9 ng/mL for P78 were calculated at 0.5 and 4 h, respectively. Ratios of the peptide levels are given at the top of the graph bars (n = 15). Values are presented as means ± SEM. (B) Western blot (4–20% gradient SDS-PAGE) using an N-terminal PEDF polyclonal antibody confirms the presence of P60 and P78 in vitreous samples (20 μL) at 0.5 and 4 h, respectively, after the eye drops were given. Endogenous PEDF was also detected in the vitreous as the usual doublet migrating at ~50 kDa (M, molecular markers). (C) Densitometric analyses of Western blots indicate the difference in levels of the P60 and P78 peptides reaching the vitreous at the time points when their highest levels are seen by fluorometric analysis (A).

Eye Drop Formulation

The human PEDF gene was redesigned according to our published methods (25) to preferentially match *Escherichia coli* codon frequencies to optimize speed and efficiency of peptide translation. After *de novo* generation, synthetic PEDF DNA was cloned into the pET32a vector, and the recombinant construct was transformed into BL21Star(DE3) cells used as a template. DNA encoding the PEDF antiangiogenic and neuroprotective fragments, PEDF60–77 (P60) and PEDF78–121 (P78), were obtained by PCR from the codon optimized sequence using the following primers: P60: 5′-GGA GGT ACC ATT GAG GGA CGC AAC TTC GGG TAC GAT CTG-3′ (forward); 5′-GGC GGA CTC GAG TTA ATT TGT GGT CGG GCT-3′ (reverse); P78: 5′- GGA GGT ACC ATT GAG GGA CGC GTG CTG CTG AGC CCG CTG TCG GTG GC-3′ (forward) and 5′-GGC GGA CTC GAG TTA GGT GCC ATG AAT GTC TGG AGA GCT-3′ (reverse). Fragments were subcloned, plasmids were expressed in BL21Star(DE3) and peptides were isolated using Ni-NTA metal affinity chromatography essentially as we have described (25). Purified peptides were cleaved from the vector's upstream thioredoxin sequence using recombinant enterokinase (rEk) and factor Xa. Sequence, molecular weight and peptide purity were confirmed by matrix-assisted laser desorption/ionization–time-of-flight (MALDI-TOF) and Western blot by using an N-terminal PEDF polyclonal antibody (made in our laboratory) that recognizes both N-terminal peptides.

Purified PEDF and its active peptide derivatives were labeled with Alexa Fluor 488 according to the manufacturer's recommendations. Conjugated peptides were dialyzed against several liters of water to remove unbound label. A sample containing unconjugated Alexa Fluor 488 was also dialyzed and served as a label control. An eye drop formula containing 1 mg/mL labeled dialyzed peptide diluted in artificial tears (Prestige Brands International) was prepared for each sample. Eye drops were administered in 5 μL (5 μg) volume onto the ocular surface of rats or diabetic mice to test distribution of the labeled peptides in the eye and to quantify levels reaching the vitreous compartment. An equal volume and concentration of dialyzed unconjugated Alexa Fluor 488 was used as a control eye drop.

Peptide Levels in the Vitreous

Adult male Sprague Dawley rats (Harlan Laboratory, Indianapolis, IN, USA) were used to test the concentration of peptides reaching the vitreous by topical delivery in eye drops. Rats were used because of the larger volume of vitreous obtained from these animals compared with the mouse eye. All animals were bred and maintained at the Penn State Hershey Medical Center in accordance with the University Institutional Animal Care and Use Committee guidelines. The 5-μL eye drops containing the peptides (5 μg) were applied to the corneal surface of rats anesthetized by intraperitoneal injections containing a mixture of 100 mg/kg ketamine and 10 mg/kg xylazine. Controls received artificial tears (ATs) containing the dialyzed free dye alone. Animals were sacrificed at time intervals between 0.5 and 8 h after treatment, eyes were enucleated and washed extensively in several changes of ice-cold phosphate-buffered saline (PBS), corneas were dissected and lens were removed. Approximately 35 μL vitreous sample was collected from each eye for fluorescence spectroscopy using the Hitachi F-2000 Fluorescence Spectrophotometer (Hitachi Instruments, Danbury, CT, USA). Samples were diluted 1:10 in PBS, and fluorescence measurements were collected at excitation and emission wavelengths of 488 and 535 nm, respectively. Concentrations were obtained by using a standard curve of dialyzed labeled peptide. Peptides in the vitreous samples (20 μL) were resolved on 4–20% gradient sodium dodecyl sulfate–polyacrylamide gel electrophoresis (SDS-PAGE) (Criterion TGX; Bio-Rad), and Western blotting was carried by using a PEDF N-terminal polyclonal antibody to examine levels of the peptides in the vitreous samples after eye drop treatments.

Eye Drop Treatments: *Ins2^{Akita}* Diabetic Mice

Hyperglycemic heterozygote C57BL/6J *Ins2^{Akita}* mice (The Jackson Laboratory, Bar Harbor, ME, USA) have a mutation in the Ins2 gene that results in hyperglycemia at ~4.5 wks of age and detectable

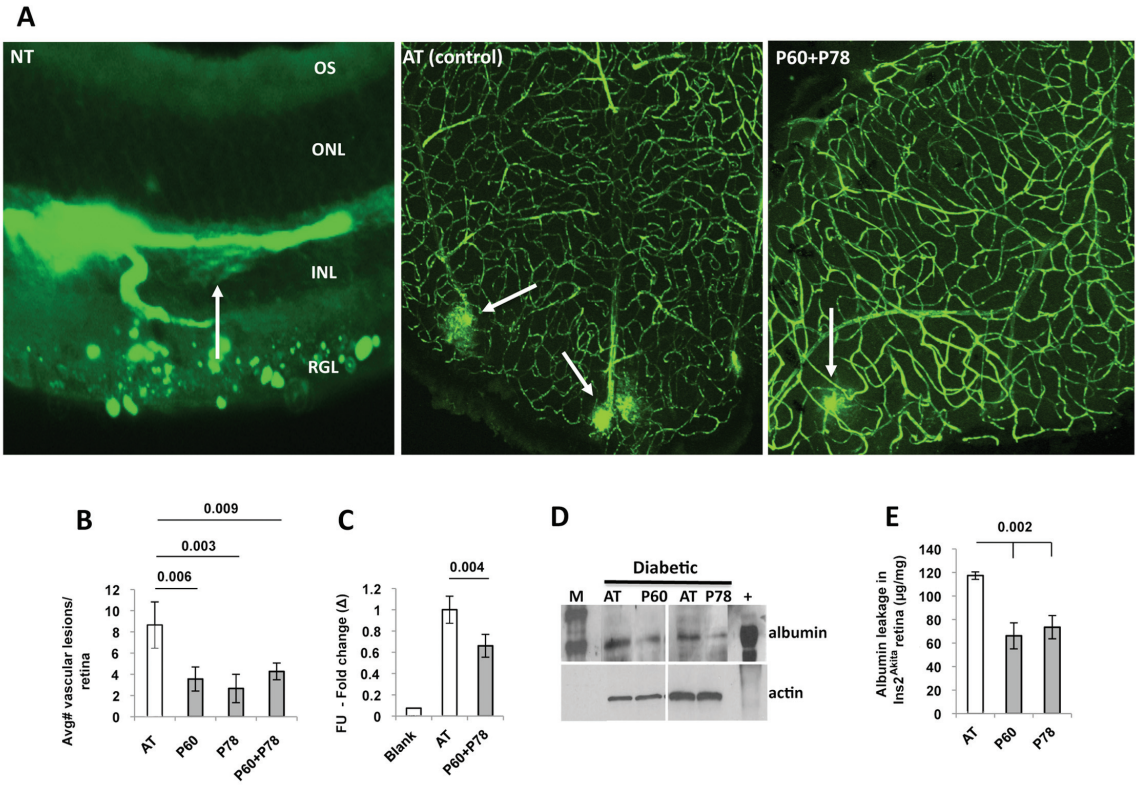

Figure 4. Reduction of vascular leakage in the diabetic *Ins2*^{Akita} mouse retina by PEDF derivatives. Retinas were evaluated 30 min after animals received tail-vein injections of BSA-FITC. (A) Left: Cross-section of a diabetic retina (NT) showing diffusion of fluorescently labeled BSA into the adjacent parenchyma of a blood vessel. The arrow points to a large vessel in the inner retina (OS, outer segment; ONL, outer nuclear layer; INL, inner nuclear layer). Middle: Control: Retina flat mount of a diabetic retina treated with vehicle alone (AT). The arrows point to several areas of BSA-FITC accumulation in the retinal parenchyma indicative of hemorrhaging. The vascular bed contains vessels that are thin and discontinuous. Right: Retina flat mount from a diabetic animal treated with the peptide eye drops. Fewer focal leakage areas and a thicker more continuous vascular bed are seen after treatment. (B) Quantitative measurements confirm that the number of hemorrhaging areas in the retina is reduced by ~55% after treatment, with either peptide or a combination of the two when compared with controls (AT) ($p < 0.05$). Differences were statistically insignificant between P60, P78 and combination treatments (n = 15). (C) Fluorometric measurements confirm a reduction in total BSA-FITC content in retina homogenates by ~40% after treatment with the PEDF derivatives compared with controls (FU, fluorescence units; $p = 0.004$). (D) Reduced levels of leaked albumin in the diabetic retina after treatment with either peptide was verified by Western blots of retina lysates (M, molecular weight standard; +, positive control – purified albumin protein). (E) Densitometry measurements of Western blots confirm a significant decrease in leaked albumin content in the peptide-treated group compared with AT controls ($p = 0.002$). Difference between P60 and P78 was statistically insignificant (n = 5). Values are means ± standard deviation (SD).

vascular complications at ~16–17 wks of age (12–13 wks of hyperglycemia). These animals were kept on a 12-h light–dark cycle, and food and water were provided *ad libitum*. Insulin was not supplemented to the diet. Heterozygote *Ins2*^{Akita} males were crossed with C57/Bl6/J females and diabetic offspring was confirmed by genotyping and blood glucose levels >250 mg/dL at 4.5 wks of age. Only male hyperglycemic mice were used, since diabetic retinopathy in females displays inconsistent pathological features. Glucose levels were measured in blood samples obtained from tail punctures by using the One-Touch LifeScan meter (LifeScan, Milpitas, CA, USA). Animals with 300–400 mg/dL serum glucose levels were used in this study.

One group of diabetic *Ins2*^{Akita} mice was treated with eye drops containing labeled peptides for 2–4 h to examine distribution of the molecules in the eye. The animals were anesthetized at specific time points by using ketamine (100 mg/kg) and xylazine (10 mg/kg) intraperitoneally, and eyes were enucleated and washed extensively in ice-cold PBS. Whole eyes or dissected retinas and corneas were fixed with 4% paraformaldehyde, embedded in O.C.T. (Tissue-Tek; Sakura, Alphen aan den Rijn, the Netherlands) and cryosectioned.

A second group of mice was used to determine effects of the peptides on diabetes-induced pathologies in the retina over a period of 15 wks of hyperglycemia. This time point was chosen because vascular pathology is easier to detect by our

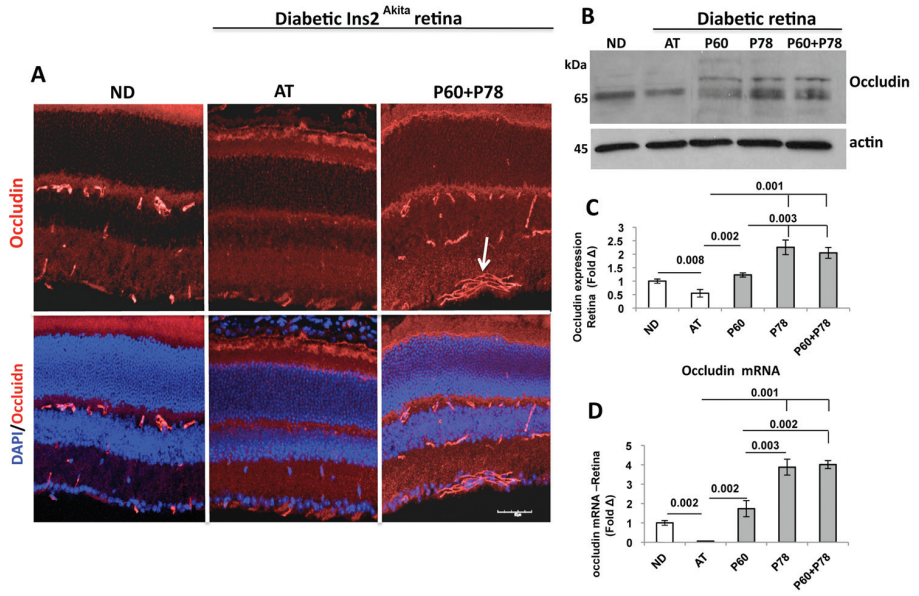

Figure 5. Regulation of occludin expression in the diabetic retina by P60 and P78. (A) The confocal images show a decrease in occludin expression in diabetic *Ins2*^{Akita} retinas (AT, vehicle treated) compared with ND controls (ND). Treatment with a combination of PEDF derivatives increased occludin expression in the retinal vasculature (arrow) of the diabetic animals (scale bar = 50 μmol/L) (n = 5). Western blot (B), densitometry measurements (C) and mRNA expression studies (D) confirm that the PEDF peptides significantly increased occludin levels in the diabetic retinas. P78 had a stronger effect than P60 in boosting both protein and mRNA expression ($p \leq 0.05$). Differences between P78 and the combination peptide treatment were statistically insignificant. *p* values are indicated in the histograms where statistical significance was observed. All values are means ± SD.

methods (beginning at ~12.5 wks). Diabetic male *Ins2*^{Akita} mice received one peptide eye drop per week for 13–15 wks immediately at the onset of hyperglycemia (4.5 wks old). Mice were manually restrained or lightly anesthetized when necessary, and 5-μL unlabeled peptides in ATs was applied to the corneal surface. This group was subdivided into four treatment groups, each receiving one of the following eye drops: P60, P78, P78 + P60 or ATs. Both eyes received the same treatment to avoid drug cross-contamination between the eyes by the animal. Animals were given 200 μL saline intraperitoneally to prevent dehydration and were placed in warmed cages to recover.

Vascular Lesions and Leakage Measurements

Vascular hemorrhaging and cell death in the retina were measured according to published time lines for the diabetic *Ins2*^{Akita} mice (4). Age- and weight-matched male C57/Bl6/J mice were used as nondiabetic (ND) controls. Anesthetized mice were given 0.5 μL BSA-FITC (100 mg/kg fluorescein isothiocyanate–bovine serum albumin) by tail vein injections. The animals were sacrificed 30 min later, and retinas were dissected, fixed and flat-mounted onto glass slides or cryosectioned to obtain optical sections by confocal microscopy. Focal vascular leakage in the retina was scored in all four retinal quadrants of flat mounts by using a 20× objective and the confocal Fluoview FV1000 software (Fluoview1000; Olympus America, Center Valley, PA, USA). Six microscopic fields were sampled in each quadrant in both the central and peripheral retina, and data were presented as the average number of lesions/retina.

In addition to visual scoring of microvascular lesions, leakage was determined by quantitative fluorescence spectroscopy (Hatachi F-2000) at excitation and emission wavelengths of 488 and 535 nm, respectively. For this analysis, retinas were dissected from treated and untreated diabetic mice after BSA-FITC injections, and each was solubilized in 300 μL ice-cold PBS. Total fluorescence in this preparation was determined by quantitative fluorimetry and presented as fold-changes to the controls. A third measurement to estimate leakage in the retina was carried out by Western blot analysis of albumin content in the retinas by using a mouse albumin antibody (1:1,000 dilution).

Gene Expression

Immunohistochemistry. Retinas were fixed in 4% (v/v) paraformaldehyde (PFA), cryopreserved in 30% sucrose and embedded in OCT, and 10 μmol/L cryosections were obtained. Nonspecific antigen binding sites were blocked with 0.5% BSA containing 10% antibody host serum for 30 min before incubation overnight at 4°C in one of the following primary antibodies: the polyclonal antibodies ZO1, occludin, IBA1 and pAKT; the monoclonal antibodies pERK and GFAP. Antibodies were diluted 1:100 to 1:200 in PBS containing 0.5% BSA and 0.5% Triton X-100. Replacement of the primary antibody with host serum served as the negative control. Cy3-conjugated goat anti-rabbit or goat anti-mouse IgGs diluted 1:2,000 in 5% BSA/PBS were used as secondary antibodies for sections labeled with polyclonal or monoclonal primary antibodies, respectively. Hoechst diluted 1:10,000 in PBS was applied to the immunolabeled tissues for 5 min, and samples were mounted on glass slides by using the *SlowFade* Gold antifade reagent (Invitrogen; Life Technologies). Fluorescence signals were evaluated visually, and optically sectioned photomicrographs were obtained by confocal microscopy (Olympus) by using the Fluoview 1000 software. Acquisition parameters for each antibody were held constant among the treatment and control groups.

Western blot. Retinas were homogenized in lysis buffer, and soluble proteins were extracted by centrifugation. For protein expression studies, 30 μg retinal extracts were separated by 10% SDS-PAGE. To detect levels of P60 and P78 reaching the vitreous after they were topically applied to the cornea, 20 μL vitreous samples were resolved on 4–20% gradient SDS-PAGE gels along with the 2–250 kDa Precision Plus Protein Dual Xtra Standards (Bio-Rad). Gels were electro-transferred for 2 h at 0.3A onto nitrocellulose membranes and nonspecific antigen binding sites blocked with 5% nonfat dried milk in Tris-buffered saline containing 0.1% Tween-20 (TBS-T; blocking buffer). Transblots were incubated overnight at 4°C with one of the following polyclonal antibodies diluted in blocking buffer: PEDF (1:1,000), ZO1 (1:1,000), occludin (1:1,000), IBA1 (1:500), AKT (1:500), pAKT (1:500), ERK1/2 (1:500), PI3K (1:500); or the monoclonal antibodies: GFAP (1:1,000); pERK1/2 (1:500), or actin (1:15,000). Membranes were then washed to remove unbound antibodies and exposed for 1 h at room temperature to either horseradish peroxidase–conjugated affinity purified goat anti-rabbit or anti-mouse IgG at 1:2,000 dilution in blocking buffer. Horseradish peroxidase activity was assessed by using the Pierce enhanced chemiluminescent Western blotting substrate followed by exposure to Kodak Scientific Imaging X-OMAT LS Film. Densitometry measurements of signals on Western blots were calculated by using the National Institutes of Health (NIH) ImageJ software (Bethesda, MD; http://rsb.info.nih.gov/ij/).

PCR. Total mRNA was isolated from controls and treated retinas and converted to first-strand cDNA by using the RNeasy reagents and the Superscript First Strand Synthesis System. Reverse transcription (RT)-PCR was carried out by using 300 ng cDNA, Taq PCR master mix and primer-specific annealing temperatures for 35 amplification cycles. Samples containing no reverse transcriptase served as negative controls to verify that amplification was cDNA and not genomic dependent. PCR products were resolved by 1% agarose gel electrophoresis. For quantitative real-time PCR, the two-step amplifying protocol was used with iQ SYBR Green Supermix solution. Both melting curve and gel electrophoretic analyses were used to determine amplicon homogeneity and quality of the reaction. Primers used in the reactions were as follows: ZO1: forward, 5′ACG ACA AAA CGC TCT ACA GG 3′, reverse, 5′ GAG AAT GGA CTG GCT TAG CA 3′; occludin: forward, 5′ CTG CTT CAT CGC TTC CTT AG 3′, reverse, 5′GGG GAT CAA CCA CAC AGT AG3′; IBA1: forward, 5′ GGA CAG ACT GCC AGC CTA AG 3′, reverse, 5′ GTT TCT CCA GCA TTC GCT TC 3′; GFAP: forward, 5′ TCC TTG TCT CGA ATG ACT CC3′, reverse, 5′ CTG TGC AAA GTT GTC CCT CT 3′.

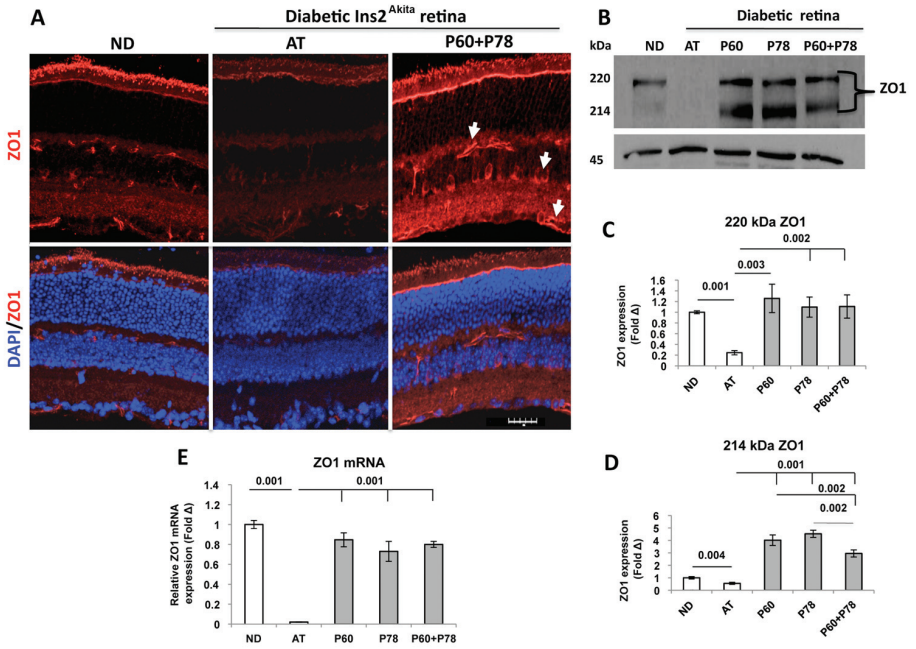

Figure 6. Regulation of ZO1 expression in diabetic retinas by P60 and P78. (A) The confocal images indicate that ZO1 expression is decreased in the retinal vasculature (arrowheads) in diabetic conditions (AT) compared with the ND retinas (ND). Increased ZO1 expression was seen in the vasculature (arrows) of the diabetic retinas after treatment with a combination of the PEDF derivatives (scale bar = 50 μmol/L) (n = 6). Western blot analysis (B) and densitometry measurements (C, D) confirm a decrease in two ZO1 isoforms (220 and 214 kDa) in the diabetic groups and an increase in their expression after treatment with P60 or P78. (E) PCR analysis provides supporting evidence that both derivatives increased ZO1 mRNA expression. Differences between P60, P78 and the combination treatment were statistically insignificant (n = 4). *p* values are indicated in the histograms where statistical significances were observed among the treatment groups. Values are means ± SD.

Peptide Signaling

In vivo. After the duration of the peptide eye drop treatments, retinas were harvested from control ND and diabetic groups receiving ATs alone (vehicle, AT) or P60 and P78 treatments for immunohistochemical processing and analyses. Retinas were fixed, embedded in OCT, cryosectioned and immunolabeled with the pAKT and pERK1/2 antibodies, as described above.

Ex vivo. Retina explants obtained from age-matched, ND male C57BL/6J mice (The Jackson Laboratory) were exposed to high glucose and used as an *ex vivo* model of diabetes to examine signals in-

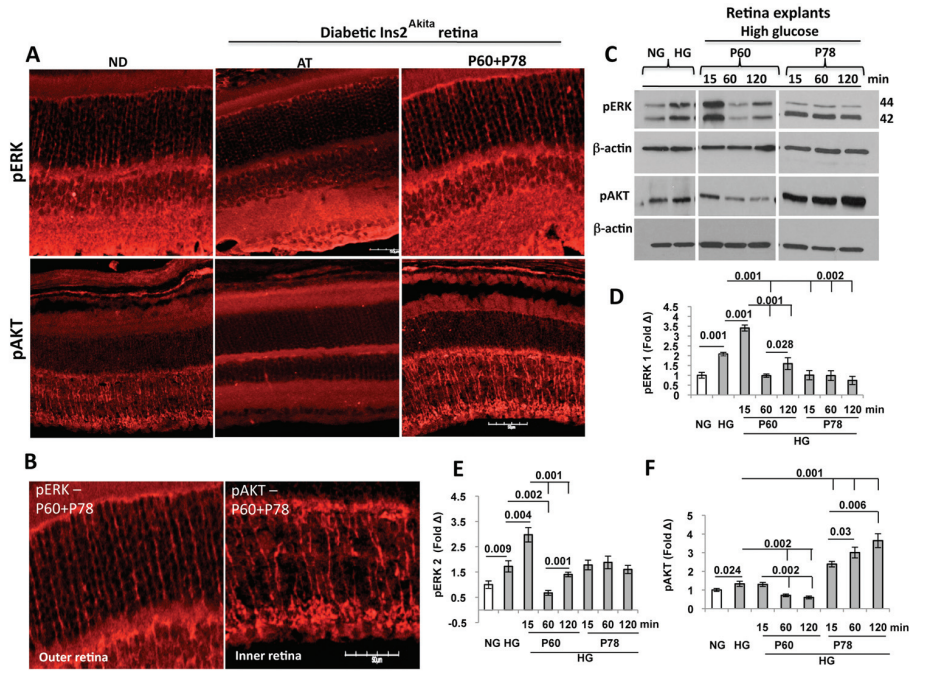

Figure 7. Modulation of ERK1/2 and AKT signaling in the diabetic retina after peptide treatment. (A) The confocal micrographs show that ERK1/2 and AKT signaling were decreased in diabetic retinas (AT) compared with ND controls (ND). Treatment with the PEDF derivatives induced activation of both ERK and AKT in diabetic retinas. Similar to the nondisease controls, ERK signaling was confined to Muller glia processes in the outer retina and AKT activation in Muller glia cell processes of the inner retina. (B) Higher magnification of the micrographs in (A) showing pERK (outer retina) and pAKT (inner retina) immunolocalization in Muller processes in animals receiving the peptide eye drops (n = 5) (scale bar = 50 μmol/L). (C) The Western blots show that ERK and AKT activation were also evident in retinal explants cultured for 24 h in high glucose (HG) (25 mmol/L) and were then treated with P60 or P78 for 15–120 min. (D, E) Densitometric analyses of the Western blots indicate that P60 induced rapid activation of ERK1/2. P78 reduced ERK1 phosphorylation below the HG controls but had no effect on ERK2 activation, and P78 (F) promoted and sustained activation of AKT throughout the treatment period (n = 3; $p < 0.05$) (NG, normal glucose). Statistically significant comparisons for P60 and P78 are indicated in the figures. All values are means ± SD.

duced by P60 and P78 in the retina and their effects on ZO1 and occludin expression. Dissected retinas were cultured in normal glucose (17.5 mmol/L) or high glucose (25 mmol/L) in DMEM containing 10% fetal bovine serum for 24 h and were then incubated at various time points between 15 and 120 min in one of the following conditions: medium alone (normal or high glucose), P60 (400 ng/mL) or P78 (400 ng/mL). Some of the explants were also treated with the pharmacological inhibitors to PI3K (iPI3K; LY294,002; 50 μmol/L), or the broad acting inhibitor to the MAP kinase pathway (iMAPK; U0126; 10 mmol/L) alone or in combination with P60 or P78 for 24 hr to examine modulations in ZO1 and occludin mRNA levels. In this case, the explants were pretreated with the inhibitors for 30 min before addition of the peptides to the cultures. Explants were harvested and protein or mRNA was extracted for Western blot and PCR analyses.

Cytokine Levels in the Vitreous: Luminex Bead Assay

The Affymetrix Procarta Cytokine assay platforms for mouse biofluids were used in conjunction with the Luminex Bio-Plex instrument (Bio-Plex 200; Bio-Rad) to obtain quantitative multiplexed measurements of cytokine levels in the vitreous. Twenty different cytokines were measured by using Luminex spectrally distinct antibody beads. Samples of 5 μL vitreous obtained from ND control groups or 15-wk vehicle-treated (AT) and peptide-treated hyperglycemic *Ins2*^{Akita} mice were bioplexed simultaneously. Samples and standards were diluted to the required volume and added to prewashed antibody-linked beads for 60 min with constant shaking at 500 rpm at room temperature. Beads were washed several times by vacuum filtration and 25 μL premixed detection antibodies added to the samples for 30 min with constant shaking at room temperature. The beads were then washed and incubated with Streptavidin-PE for 30 min at room temperature, and data were collected by using the Luminex Acquisition software, Bioplex Manager Version 4.11 (Bio-Rad). Relative amounts of cytokines were calculated by using standard curves generated from reference concentrations supplied by the manufacturer and quantitative data were expressed in pg/mL ± standard error of the mean (SEM), with $p < 0.05$ taken as statistically significant.

Morphometric Analysis

Retina cryosections were stained with propidium iodide (PI) to examine cell dropout in the retinal ganglion layer (RGL). Comparisons were made among retinas obtained from the following groups of animals: ND controls and diabetic: no treatment (NT), vehicle-treated (AT), P60, P78 and combination peptide-treated groups. Cryosections were treated with 4 ng/mL PI diluted in PBS for 30 min at room temperature. Samples were washed with PBS and mounted, and the nuclear staining in the retina was assessed by confocal microscopy. Because the sections were fixed, the nuclei in all retinal layers were stained red. Three serially obtained PI-treated paraffin sections from each eye were used for morphometric analysis. The sections were spaced 20 μmol/L apart, and the

number of PI-stained cells in the retinal ganglion cell (RGC) layer and thickness of the inner plexiform layer (IPL) were evaluated in all retinal eccentricities using high-resolution confocal optical slices. Cell counts and IPL measurements were taken from 6 × 250 μmol/L zones along the full length of the retina from centrally located fields adjacent to the optic nerve to peripheral regions. Eighteen fields were analyzed per retina. Images of optical sections were acquired by using an Olympus Fluoview FV 1000 confocal microscope equipped with a 20× objective. The number of stained nuclei in the RGC layer was counted, and data are presented as the average number of cells/100 μm in each treatment group. The margins of the IPL were defined by the RGC layer and inner nuclear layer of the retina. IPL measurements were taken centrally and peripherally from the border between the inner nuclear layer and the ganglion cell layer to the border between the IPL and the inner nuclear layer according to our published work (24), and the data are presented as mean thickness of the IPL.

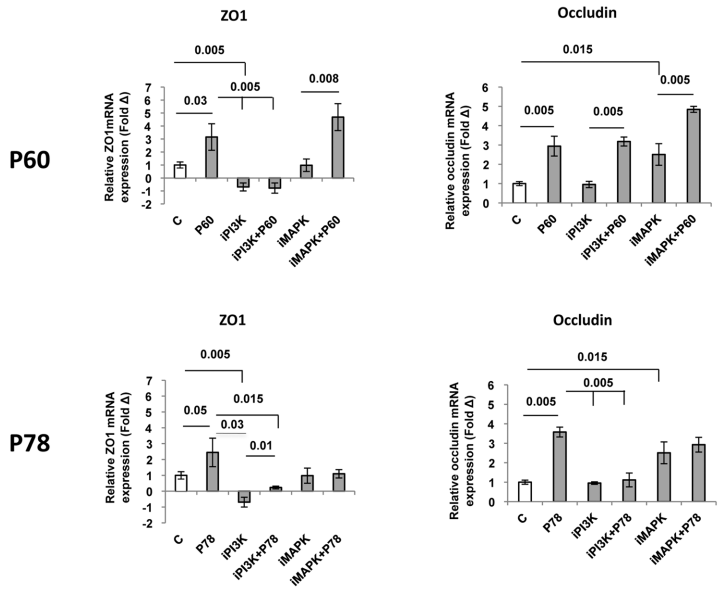

Figure 8. Regulation of ZO1 and occludin expression by the PEDF derivatives through the PI3K/AKT pathway. Quantitative PCR measurements indicate that the effects of P60 and P78 on ZO1 and occludin expression are mediated through the PI3K/AKT pathway in a retinal explant model of diabetes. Explants were cultured in high glucose (25 mmol/L) for 24 h in the presence/absence of the pharmacological inhibitors of PI3K (iPI3K; LY294,002), MAPK (iMAPK; U0126) and one or the other of the PEDF derivatives (n = 4). iPI3K blocked P78 effects on both ZO1 and occludin expression. It also inhibited the effects of P60 on ZO1 expression but not on occludin levels. *p* values are indicated for statistically significant comparisons. All values are means ± SD.

Statistical Analysis

All experiments were repeated at least three times in triplicate for *in vitro* studies, and at least five animals were used for *in vivo* analyses. Statistical analysis was performed by using the Prism 5 GraphPad Software (La Jolla, CA, USA), and quantitative data were obtained by using a Student *t* test (two-tailed, unpaired) to compare two groups and one-way analysis of variance (with a Newman-Keuls *post hoc* test) to compare more than two groups. Densitometry analyses were performed by using the NIH ImageJ software. Results are expressed as mean ± SEM. $p < 0.05$ was statistically significant. Values are given above graph bars for comparisons showing statistical significance.

RESULTS

Peptide Expression and Purification

Two PEDF derivatives containing the antiangiogenic (P60) (26) and the neuroprotective (P78) (24, 27) activity of the parent polypeptide (22,23) were expressed at high levels by using a synthetic codon optimized PEDF gene sequence (25). Purity and size of P60 at 2.1 kDa and P78 at 4.7 kDa were confirmed by SDS-PAGE and by Western blot analyses by using a PEDF polyclonal antibody. Yields of purified P60 and P78 peptides after removal of the upstream thioredoxin vector sequence were 14.8 and 17.1 mg/L, respectively (Figure 1 and Table 1).

Distribution of Labeled PEDF Derivatives in the Eye

In cross-sections of the whole eye receiving eye drops, fluorescence signal for Alexa Fluor–labeled P60 and P78 formulated in ATs was visible in the cornea, ciliary body, retinal pigment epithelium (RPE)-choroid complex and various retinal layers within 2 h of topical application (Figure 2A). Penetration of labeled P60 across the corneal epithelium occurred within the first 60 min with near completion by 2 h (Figure 2B). Penetration of P78 was visibly slower than P60. It was clearly visible by 2 h, and a residual amount was still seen at the corneal surface by 4 h. The full-length parent PEDF (50 kDa) remained largely at the ocular surface with trace amounts visible in the corneal endothelium 2–4 h after the eye drops were administered. The dialyzed unconjugated label (control) was barely visible in the cornea or retina and served as a label control in the study. In the posterior eye, both peptides were detected in the vitreous, vasculature of the inner retina and those vessels invading the vitreous, and in some cells throughout the diabetic retina. The labeled peptides were also prominent in the RPE-choroid complex (Figure 2C).

Confirmation that the PEDF derivatives were delivered to the retina in eye drops was obtained by quantitative fluorescence

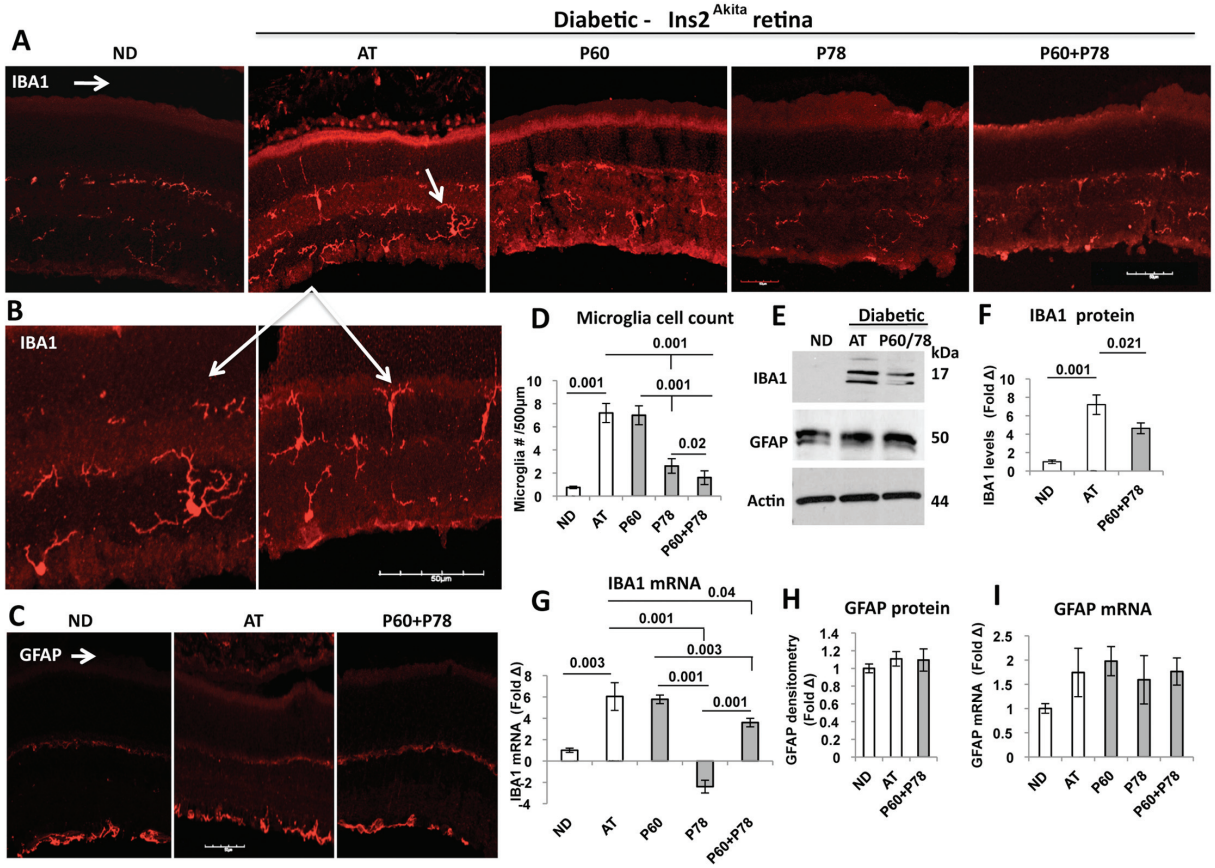

Figure 9. Reduction in glia activation in diabetic retinas by P78. (A) The confocal images show an increase in numbers of IBA1-labeled activated microglia in the *Ins2*^{Akita} diabetic retinas (AT) compared with retinas from ND mice (ND). P78 or the combination peptide treatment reduced numbers of reactive microglia in the diabetic retina. P60 had no effect on the activation of these cells. The arrow in the control (AT) indicates large amoeboid-like microglia expressing the IBA1 marker in the inner retina. (B) Higher magnification of the control from (A) showing ramifications of large microglia in the inner retina. (C) GFAP expression was detected in astrocytes and not in Muller glia cells in controls and treated and untreated samples (scale bar = 50 µmol/L). (D) Cell counts confirm that P78 reduced microglia activation in the diabetic retina by ~60% (p = 0.001). The difference between AT and P60 treatment was statistically insignificant (n = 8). Western blot (E) and densitometry measurements (F) confirm an increased in IBA1 levels and a reduction after treatment in diabetic retinas. (G) mRNA levels in the retina provide supporting evidence that P78 reduced microglia activation in diabetic conditions (p = 0.001) (n = 3). Densitometry measurements of Western blots (H) and quantitative PCR (I) indicate that GFAP protein and mRNA levels were not altered with diabetes. Comparisons among the peptide- and vehicle-treated groups where p values are not indicated in the graphs are statistically insignificant. All values are means ± SD.

spectroscopy and Western blot analyses (Figure 3). Peak levels of each peptide were detected in the vitreous at different time points, with the highest levels of ~0.2 µg/mL at 0.5 h and 0.9 µg/mL at 4 h for P60 and P78, respectively. A polyclonal antibody to the N-terminal region of PEDF recognized both peptides in vitreous samples after they were applied to the corneal surface as well as endogenous PEDF, which is present in the normal vitreous (22). Quantitative measurements on Western blots of peptide levels in the vitreous confirm fluorimetric ratios for P60 and P78 (~1:4 ratio) at 0.5 and 4 h, respectively, after treatment.

Vascular Pathology

The effects of eye drops containing unlabeled PEDF derivatives were evaluated on vascular hemorrhaging in the diabetic *Ins2*^{Akita} retina. Increased BSA-FITC, given by tail vein injections, visibly leaked into the retinal parenchyma surrounding several lesioned areas (Figure 4). Gross thinning of the vascular bed was also noted in the control vehicle (AT)-treated retinas. There was a reduction in the number of vascular hemorrhaging areas by ~60%, BSA-FITC extravasation by ~30% and leaked albumin content by ~45% in the peptide-treated retinas compared with vehicle-treated controls. Together, these analyses confirm that both peptides were delivered to the retina in eye drops at doses that diminished the extent of vascu-

lar leakage in the tissue. Significant differences on vascular leakage were not observed between the individual peptides.

Regulation of Tight Junction Proteins

Because we noted a decrease in vascular leakage in the retina by these PEDF derivatives, we examined their effects on expression of two tight junction proteins, occludin and ZO1, which are reported to be associated with vascular permeability (15,16). In the diabetic animals, there was relatively weak occludin (Figure 5) and ZO1 (Figure 6) expression in the vasculature of the inner retina compared with high levels in the ND groups. The PEDF derivatives increased levels of both tight junction proteins in the inner retina vasculature of the diabetic retinas. These changes were confirmed by Western blot and PCR analyses as well. Whereas both peptides were effective in increasing expression of these tight junction proteins, P78 had a stronger effect on boosting occludin protein and mRNA levels ($p = 0.001$) (Figure 5). ZO1 migrated as two isoforms of molecular weight 214 and 220 on Western blots. The lower molecular weight protein was barely visible in the ND retinas, both were significantly reduced in the diabetic retinas and treatment with either of the PEDF peptides increased levels of both isoforms ($p < 0.05$). Increased expression of ZO1 mRNA levels by the peptides was also confirmed by PCR analysis ($p = 0.001$) (Figure 6).

Activation of AKT and ERK1/2 Signaling in Muller Glia

In the normal retina, Muller glia expressed high levels of pAKT and moderate levels of pERK1/2 in their radial processes spanning the retina. ERK1/2 signaling was evident in Muller fibers that span the outer retina and was also detected in cells of the outer plexiform layer and inner retina. pAKT signaling was mostly confined to Muller fibers of the inner retina (Figure 7). In the diabetic condition, both pAKT and ERK1/2 signaling was dampened in the Muller glia processes. Treatment with a combination of the peptides activated both signals in Muller glia fibers similar to levels seen in the nondiseased retinas.

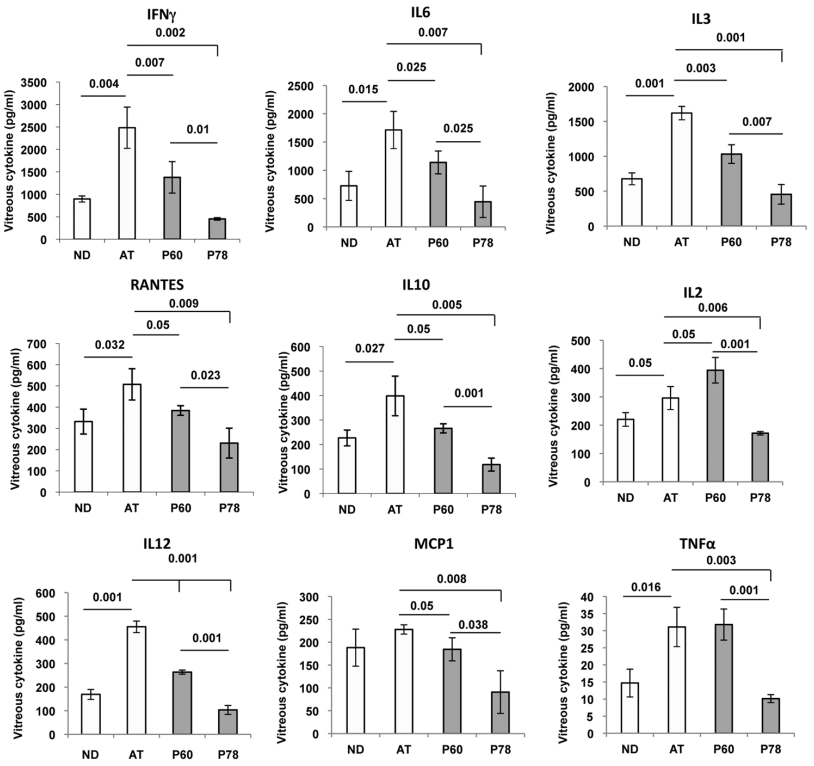

Figure 10. Reduction in inflammatory cytokine levels in the diabetic vitreous after treatment with P60 and P78 peptide eye drops. The histograms represent Affymetrix Luminex bead measurements of cytokine levels in the vitreous. An increase in 8/20 inflammatory cytokines was detected in the diabetic condition compared with the normal controls. Both of the PEDF derivatives reduced vitreous levels of these cytokines, but maximal effect was seen after P78 treatment. Only P78 reduced TNFα ($p = 0.003$) and IL2 ($p = 0.006$) levels (n = 5). All values are means ± SD.

To examine which of these peptides regulated the AKT and MAPK pathways, we used an *ex vivo* model of diabetes, in which retinas were cultured in high glucose conditions supplemented with one or the other peptide for 15–120 min (Figure 7). P60 transiently enhanced phosphorylation of ERK1/2 (44/42) and rapidly decreased AKT activation by 15 min. P78, on the other hand, rapidly decreased and maintained lower phosphorylation levels of ERK1 (44 kDa), had no effect on ERK2 (42-kDa protein) and boost activation of AKT over the course of the treatment (Figure 7). Our results indicate that P78 induces pAKT and P60 promotes pERK1/2 signaling in Muller glial and suggests that these cells may play an important role in the pathogenesis of diabetic retinopathy through mechanisms involving these signaling pathways.

Expression of Occludin and ZO1 in the Retina through the PI3K/AKT Pathway

On the basis of the findings above, we further investigated whether a correlation existed between activation of these pathways in Muller glia and regulation of the two tight junction proteins in inner retina vasculature by the PEDF derivatives. By using pharmacological inhibition of the MAPK (U0126) and PI3K/AKT (LY294,002) pathways in retina explants exposed to high glucose, we confirmed that P60 and P78 induced expression of ZO1 and occludin and demonstrated that P78 induced their expression through activation of the PI3K/AKT pathway (Figure 8). P60 activated ZO1 expression through the

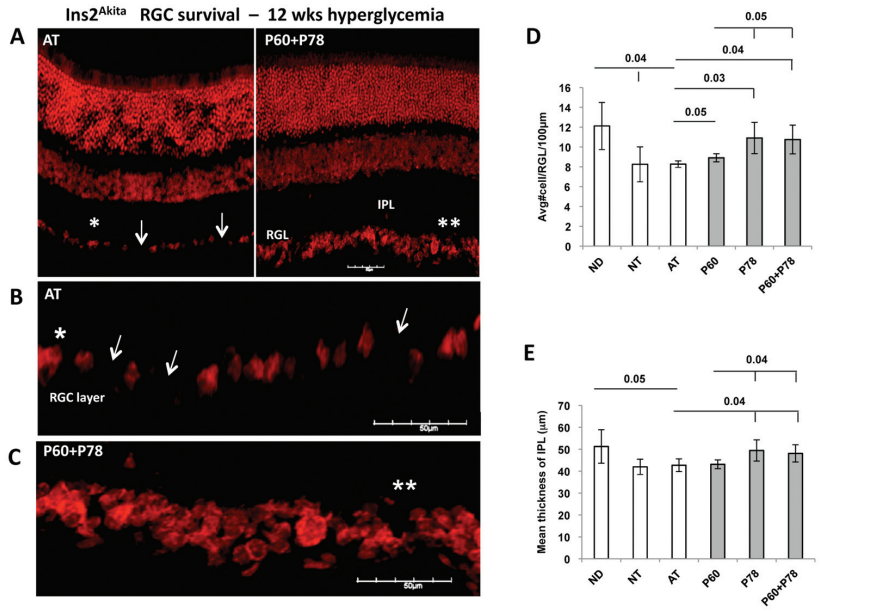

Figure 11. Neuronal protection in diabetic retinas by P78. (A) Nuclear staining of fixed retinas with PI showing the various nuclear layers in the control vehicle (AT) and peptide-treated diabetic retinas. A loss of cells in the RGL (arrows) was noted in the diabetic condition and a reduction in cell drop out in the peptide-treated retinas. (B, C) Higher magnification of the RGL in the diabetic control (*) and treated (**) samples in (A) showing cell dropout (arrows) in the RGL in controls compared with the treated groups (scale bar = 50 μmol/L). (D) Cell counts confirm a loss of cells in the RGL in diabetic retinas (p = 0.04) (ND versus NT) and cell rescue after treatment with P78 (p = 0.03). (E) Measurements of the mean thickness of the IPL also indicate that P78 was effective in reducing IPL thinning (p = 0.04). The difference between AT and P60 was insignificant (n = 12). All values are means ± SD.

PI3K/AKT pathway as well, but its regulation of occludin expression was less clear.

Inflammation: Microglia, Muller Glia and Cytokines

Scattered in the diabetic retina were several large amoeboid-like microglia that upregulated expression of the IBA1 protein, a marker molecule for activated microglia (Figure 9). These were predominantly evident in the inner retina, where they extended ramifications in the retinal ganglion and inner plexiform layers. In contrast, activated microglia were rarely found in the retinas of the control ND mice and in diabetic animals that were treated with P78 or a combination of the peptides. Cell counts confirmed that P78 reduced the numbers of activated microglia in the diabetic retina by ~60% (p = 0.001) compared with the diabetic controls. Western blot analyses also indicated that IBA1 protein expression was increased in the diabetic retinas and that peptide treatments reduced its levels. Quantitative PCR supported the immunohistochemistry findings that the neuroprotective P78 PEDF derivative reduced diabetes-induced activation of microglia in the retina. Treatment with P60 alone had no effect on the number of activated microglia or IBA1 mRNA expression. Our studies also demonstrate that diabetes did not activate Muller glia, since expression of GFAP, a molecular signature of reactive Muller glia, was not detected in these cells in either normal, diabetic or peptide-treated retinas. GFAP expression was confined to and remained unchanged in astrocytes of the retinal ganglion cell layer.

When levels of cytokines were measured in the vitreous, 8 of the 20 studied were elevated in diabetic eyes compared with ND eyes (Figure 10). The most significant increases were for interferon (IFN)-γ, interleukin (IL)-6, IL-3, IL-12 and tumor necrosis factor (TNF)-α. P60 reduced levels of six of these eight cytokines, and P78 reduced expression of all eight and also reduced MCP1 below control levels. In all cases, the effect of P78 was greater than P60, and only P78 reduced TNFα and IL-2 content in the diabetic vitreous.

Taken together, we demonstrate that diabetes altered the inflammatory environment in the retina. It promoted an increase in microglia but not Muller glia activation and concomitantly higher levels of cytokine production in the retina. P78 reduced the number of reactive microglia, and both peptides lowered vitreous cytokine levels in the diabetic retina.

Cell Loss in the RGL

Another feature of diabetic retinopathy is loss of neurons in the RGL. We confirmed that there was a decrease in numbers of cells in the RGL and in mean thickness of the IPL in diabetic retinas by ~31 and ~17%, respectively, compared with the ND group and showed that treatment with a combination of the peptides reduced the loss of cells in the RGL (Figure 11). However, when individual peptides were tested, cell dropout was reduced by ~22% after P78 treatment, and there was no significant effect on RGC loss after treatment with P60. Measurements of the IPL indicated that P78 also increased IPL thickness by ~13% compared with retinas receiving ATs or P60.

In summary, we have shown that bioactive PEDF peptide derivatives can be delivered to the retina in an eye drop formulation at doses that alter hallmark retinal pathology in diabetic conditions. Both peptides reduced vascular hemorrhaging, promoted Muller glia signaling but not their activation, increased expression of tight junction proteins in retinal vasculature and reduced cytokine levels in the vitreous. The P78 PEDF derivative

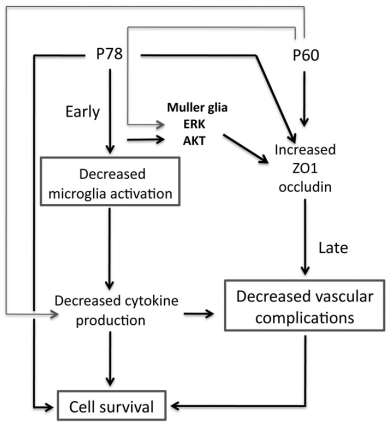

Figure 12. The schematic represents key events regulated by P60 and P78 that may reduce complications in diabetic retinopathy. The antiangiogenic P60 may reduce vascular leakage by increasing tight junction proteins in retina vessels through Muller glia signaling and by lowering levels of inflammatory cytokines that promote vessel abnormalities. Inhibition of vascular pathology could in turn have downstream effects on retina cell survival. The neuroprotective P78 derivative may reduce RGC loss in the diabetic retina by reducing early microglia activation and levels of inflammatory cytokines such as TNFα. It may block late-stage vascular leakage through a Muller glia-mediated upregulation of tight junction proteins in the retina microvasculature. P78 could also have direct effects on RGC survival by yet undefined mechanisms.

reduced microglia activation, decreased production of TNFα and IL-2 and reduced loss of cells in the inner retina. Mechanisms of how an antiangiogenic and a neuroprotective derivative of PEDF may connect pathological features of diabetic retinopathy are summarized in the schematic of Figure 12.

DISCUSSION

The effects of PEDF on cell survival and angiogenesis are well established. The 50-kDa PEDF polypeptide is endogenous to almost all tissues in the body, where its function is associated, for the most part, with neuroprotection and/or the prevention of abnormal vessel growth (22,23). Here we show that two small bioactive PEDF derivatives can be delivered to the retina when applied to the surface of the eye in doses that alter retinal biochemistry and reduce diabetic complications. The topically applied peptides were found in measurable quantities in the vitreous and are most likely delivered to this compartment through different routes, including diffusion through the cornea and the subconjunctiva, structures that showed intense fluorescence with the labeled peptides. Detection of the labeled peptides in the RPE-choroid complex and inner retina vasculature also argues for a vascular route of delivery to these structures possibly through diffusion into ocular surface vessels.

Differences in diffusion rates between P60 and P78 across the ocular surface may be due in part to peptide size, sequence and clearance. Only a trace amount of the larger PEDF was visible in the corneal endothelium, supporting arguments that large native polypeptides are poor candidates for topical delivery to the retina. Biochemical alterations in retinal signaling and vitreous cytokine levels after treatment were a good indication that therapeutic doses of the peptides were delivered to the vitreous and retina. Lower levels of P60 in the vitreous compartment compared with levels of the larger P78 peptide may be due in part to rapid clearance of P60 in the aqueous because of its size. In both cases, however, the amounts of each peptide reaching the retina were well above or equivalent to published therapeutic doses for these molecules (25–27).

A hallmark feature of diabetic retinopathy is vascular leakage. Both derivatives were effective in reducing the number of vascular hemorrhaging sites and extent of BSA-FITC leakage in the retina possibly through upregulation of tight junction proteins in inner retina vessels. Our observations that diabetes decreased retinal vessel levels of occludin and ZO1, two proteins associated with vascular permeability (15,16), and concurrently reduced AKT and ERK1/2 signaling in Muller glia and that the PEDF peptides blocked both events simultaneously suggest that these occurrences are linked. The AKT and MAPK pathways are two molecular tracks that are quite sensitive to homeostatic fluctuations in the retina (28–31). These findings implicate Muller glia in mechanisms that control vascular function, which is not surprising, since the processes of these cells are in close contact with endothelial cells lining blood vessels. Therefore, they may exert influence on junctional composition and structure in retinal vessels by molecular signals propagated through these pathways. In support of this hypothesis, we showed that pharmacological inhibition of the PI3K/AKT pathway in the retina reduced ZO1 and occludin levels and blocked their synthesis by the PEDF derivatives.

Although both PEDF derivatives were equipotent in their regulation of vascular leakage, this was not true for their effects on cell loss in the RGL, another feature of diabetic retinopathy. P78 was more effective in preventing cell dropout and IPL thinning, which may be due in part to its specific actions in reducing microglia activation, decreasing vitreous levels of TNFα and IL2 and activation of the PI3K/AKT pathway in Muller glia. P78 showed stronger effects than P60 in reducing vitreous levels of other inflammatory cytokines including IFN-γ, IL-3 and IL-6 to below baseline, which may also account for its protective effects. We cannot preclude the possibility that P78 directly blocked diabetes-induced death signals in RGCs or that its effects on neuronal survival is through upregulation of Muller glia pAKT neuroprotective signaling, since these cells are known to support neurons in the RGC layer.

Like other neurodegenerative processes, inflammation is a concurrent facet in the development of diabetic retinopathy. Measurements of visual function including contrast sensitivity, color vision and focal ERG show functional impairment long before signs of vasculopathy are detected (32–38), and histological preparations indicate a concomitant increase in microglia activation

during early stages of the disease (39). Normally quiescent microglia can become hyperactivated by inflammatory cytokines such as IFN-γ, TNFα, IL-3 and IL-6 (40–42). These cells, in turn, secrete some of the same cytokines that activate them as well as molecules that promote vascular permeability such as VEGF, IL-1β, IL-6, nitric oxide and matrix metalloproteinases (MMPs) (43–45) and factors that promote neuronal degeneration including lymphotoxins, TNFα, reactive oxygen species and glutamate (40,46,47). Thus, microglia control vascular junction stability, microaneurysm development and neuronal degeneration (6,49–52) and are a candidate perpetrator in the development of several central nervous system diseases, including Parkinson disease, aging, Alzheimer disease and HIV dementia (40,48).

How retinal microglia are activated in early stages of diabetes is not entirely clear, but activation may be triggered by glucose-induced fluctuations in homeostatic mechanisms in the retina. In the diabetic *Ins2*^{Akita} retina, RGC death begins immediately after or in parallel with microglia activation and followed by detectable vascular complications approximately 2 months downstream of the pathology (4). The timeline for these events raises questions about the extent of microglia involvement in RGC death and vascular pathology. It must be noted that, whereas P60 increased expression of tight junction proteins and blocked vascular hemorrhaging, it had no effect on microglia activation and RGC survival. P78, on the other hand, prevented microglia activation and RGC dropout, and since treatment was given before these events occurred, it is tempting to speculate that promotion of its neuroprotective effects upstream, vascular stability downstream and its apparent effects on Muller glia vascular signaling involve antiinflammatory mechanisms. This scenario argues for a microglia–Muller glia interaction in diabetic retinopathy and suggests that vascular function and neuronal survival may have a primary root in microglia activation.

CONCLUSION

In summary, we present evidence that small therapeutic PEDF derivative can be delivered to the retina in eye drop preparations, a strategy that represents an effective and less invasive way to treat diabetic retinopathy and other retinal diseases. We have used the neuroprotective and antiangiogenic PEDF peptides to dissect mechanisms of cell death and vascular pathology and found that the neuroprotective peptide reduced early inflammatory processes, cell death and downstream vascular complications of the disease that strongly suggest that these processes have a common mechanistic root. We support arguments that inflammation is a key event in diabetic retinopathy, with pathological tentacles extending to mechanisms that control vascular function and neurodegenerative processes. We suggest that there is a microglia–Muller glia interaction in the development of diabetic retinopathy and that these glia cells are key regulators of the disease progression. Our data highlight the importance of including neuroprotective and/or antiinflammatory approaches in diabetic retinopathy and other retinal degenerations with vascular complications.

ACKNOWLEDGMENTS

The authors are indebted to current and past members of the laboratory for technical assistance, discussions and investigations that contributed to this article. This work was supported by the Juvenile Diabetes Research Foundation, the David Woods Kemper Memorial Foundation, the Penna Lions Eye Research and Sight Conservation and the Penn State Frontiers in Eye and Vision Research (FEVR) award.

DISCLOSURE

The authors declare that they have no competing interests as defined by *Molecular Medicine*, or other interests that might be perceived to influence the results and discussion reported in this paper.

REFERENCES

1. Calcutt NA, Cooper ME, Kern TS, Schmidt AM. (2009) Therapies for hyperglycaemic-induced diabetic complications: from animal models to clinical trials. *Nat. Rev.* 8:417–29.
2. Barber AJ, *et al.* (1998) Neural apoptosis in the retina during experimental and human diabetes: early onset and effect of insulin. *J. Clin. Invest.* 102:783–91.
3. Scott TM, Foote J, Peat B, Galway G. (1986) Vascular and neural changes in the rat optic nerve following induction of diabetes with streptozotocin. *J. Anat.* 144:145–52.
4. Barber AJ, *et al.* (2005) The Ins2Akita mouse as a model of early retinal complications in diabetes. *Invest. Ophthalmol. Vis. Sci.* 46:2210–8.
5. Frank RN. (2004) Diabetic retinopathy. *N. Engl. J. Med.* 350:48–58.
6. Gardner TW, Antonetti DA, Barber AJ, LaNoue KF, Levison SW. (2002) Diabetic retinopathy: more than meets the eye. *Surv. Ophthalmol.* 47 (Suppl. 2):S253–62.
7. Sandoval DA, Obici S, Seeley RJ. (2009) Targeting the CNS to treat type 2 diabetes. *Nat. Rev.* 8:386–98.
8. Rask-Madsen C, King Gl. (2010) Kidney complications: factors that protect the diabetic vasculature. *Nat. Med.* 16:40–1.
9. Gao BB, *et al.* (2007) Extracellular carbonic anhydrase mediates hemorrhagic retinal and cerebral vascular permeability through prekallikrein activation. *Nat. Med.* 13:181–8.
10. Gardner TW, Antonetti DA. (2007) A prize catches for diabetic retinopathy. *Nat. Med.* 13:131–2.
11. Ruberte J, *et al.* (2004) Increased ocular levels of IGF-1 in transgenic mice leads to diabetes-like eye disease. *J. Clin. Invest.* 113:1149–57.
12. Yamagishi S, *et al.* (2006) Pigment epithelium-derived factor inhibits advanced glycation end product-induced retinal vascular hyperpermeability by blocking reactive oxygen species-mediated vascular endothelial growth factor expression. *J. Biol. Chem.* 281:20213–20.
13. Zhang SX, Wang JJ, Gao G, Parke K, Ma JX. (2006) Pigment epithelium-derived factor downregulates vascular endothelial growth factor (VEGF) expression and inhibits VEGF-VEGF receptor 2 binding in diabetic retinopathy. *J. Mol. Endocrinol.* 37:1–12.
14. Stellmach V, Crawford S, Zhou W, Bouck N. (2001) Prevention of ischemia-induced retinopathy by the natural ocular antiangiogenic agent pigment epithelium-derived factor. *Proc. Natl. Acad. Sci. U. S. A.* 98:2593–7.
15. Antonetti DA, *et al.* (1998) Vascular permeability in experimental diabetes is associated with reduced endothelial occludin content: vascular endothelial growth factor decreases occludin in retinal endothelial cells: Penn State Retina Research Group. *Diabetes* 47:1953–9.
16. Antonetti DA, Barber AJ, Hollinger LA, Wolpert EB, Gardner TW. (1999) Vascular endothelial growth factor induces rapid phosphorylation of tight junction proteins occludin and zonula oc-

cluden 1: a potential mechanism for vascular permeability in diabetic retinopathy and tumors. *J. Biol. Chem.* 274:23463–7.
17. Geraldes P, *et al.* (2009) Activation of PKC-delta dn SHP-1 by hyperglycemia causes vascular cell apoptosis and diabetic retinopathy. *Nat. Med.* 15:1298–306.
18. Tong Z, *et al.* (2008) Promoter polymorphism of the erythropoietin gene in severe diabetic eye and kidney complications. *Proc. Natl. Acad. Sci. U. S. A.* 105:6998–7003.
19. Tamarat R, *et al.* (2003) Blockage of advanced glycation end-product formation restores ischemia-induced angiogenesis in diabetic mice. *Proc. Natl. Acad. Sci. U. S. A.* 100:8555–60.
20. Gariano RF, Gardner TW. (2005) Retinal angiogenesis in development and disease. *Nature.* 438:960–6.
21. Antonetti DA. (2009) Eye vessels saved by rescuing their pericyte partners. *Nat. Med.* 15:1248–9.
22. Tombran-Tink J, Barnstable CJ. (2003) PEDF: a multifaceted neurotrophic factor. *Nat. Rev. Neurosci.* 4:628–36.
23. Tombran-Tink J, Barnstable CJ. (2003) Therapeutic prospects for PEDF: more than a promising angiogenesis inhibitor. *Trends Mol. Med.* 9:244–50.
24. Li H, *et al.* (2006) A PEDF N-terminal peptide protects the retina from ischemic injury when delivered in PLGA nanospheres. *Exp. Eye. Res.* 83:824–33.
25. Gvritishvili AG, Leung, KW, Tombran-Tink J. (2010) Codon preference optimization increases heterologous PEDF expression. *PLoS One.* 5:e15056.
26. Mirochnik Y, Aurora A, Schulze-Hoepfner FT, Deabes A. (2009) Short pigment epithelial-derived factor-derived peptide inhibits angiogenesis and tumor growth. *Clin. Cancer Res.* 15:1655–63.
27. Bilak MM, *et al.* (2002) Identification of the neuroprotective molecular region of pigment epithelium-derived factor and its binding sites on motor neurons. *J. Neurosci.* 22:9378–86.
28. Tomlinson DR, Gardine NJ. (2008) Glucose neurotoxicity. *Nat. Rev. Neurosci.* 9:36–45.
29. Purves T, *et al.* (2001) A role for mitogen-activated protein kinases in the aetiology of diabetic neuropathy. *FASEB J.* 15:2508–14.
30. Tomlinson DR. (1999) Mitogen-activated protein kinases as glucose transducers for diabetic complications. *Diabetologia.* 42:1271–81.
31. Lawrence MC, *et al.* (2008) The roles of MAPKs in disease. *Cell Res*. 18:436–42.
32. Garner A. (1993) Histopathology of diabetic retinopathy in man. *Eye.* 7:250–3.
33. Di Leo MA, *et al.* (1992) Nonselective loss of contrast sensitivity in visual system testing in early type I diabetes. *Diabetes Care.* 15:620–5.
34. Dosso AA, *et al.* (1996) Risk factors associated with contrast sensitivity loss in diabetic patients. *Graefes Arch. Clin. Exp. Ophthalmol.* 234:300–5.
35. Harris A, *et al.* (1996) Hyperoxia improves contrast sensitivity in early diabetic retinopathy. *Br. J. Ophthalmol.* 80:209–13.
36. Hardy KJ, Lipton J, Scase MO, Foster DH, Scarpello JH. (1992) Detection of colour vision abnormalities in uncomplicated type 1 diabetic patients with angiographically normal retinas. *Br. J. Ophthalmol.* 76:461–4.
37. Hardy KJ, Scarpello JH, Foster DH, Moreland JD. (1994) Effect of diabetes associated increases in lens optical density on colour discrimination in insulin dependent diabetes. *Br. J. Ophthalmol.* 78:754–6.
38. Arden GB, *et al.* (1986) Pattern electroretinograms become abnormal when background diabetic retinopathy deteriorates to a preproliferative stage: possible use as a screening test. *Br. J. Ophthalmol.* 70:330–5.
39. Rungger-Brändle E, Dosso AA, Leuenberger PM. (2000) Glial reactivity, an early feature of diabetic retinopathy. *Invest. Ophthalmol. Vis. Sci.* 41:1971–80.
40. Block ML, Zecca L, Hong JS. (2007) Microglia-mediated neurotoxicity: uncovering the molecular mechanisms. *Nat. Rev. Neurosc.* 8:57–69.
41. Suzumura A, Sawada M, Yamamoto H, Marunouchi T. (1990) Effects of colony stimulating factors on isolated microglia in vitro. *J. Neuroimmunol.* 30:111–20.
42. Basu A, Krady JK, Enterline JR, Levison SW. (2002) Transforming growth factor beta1 prevents IL-1beta-induced microglial activation, whereas TNFalpha- and IL-6-stimulated activation are not antagonized. *Glia.* 40:109–20.
43. Langmann T. (2007) Microglia activation in retinal degeneration. *J. Leukoc. Biol.* 81:1345–51.
44. Sayyah M, Javad-Pour M, Ghazi-Khansari M. (2003) The bacterial endotoxin lipopolysaccharide enhances seizure susceptibility in mice: involvement of proinflammatory factors: nitric oxide and prostaglandins. *Neuroscience.* 122:1073–80.
45. Adamis AP, D'Amato RJ. (1995) Shedding light on diabetic retinopathy. *Ophthalmology*. 102:1127–8.
46. Venters HD, *et al.* (1999) A new mechanism of neurodegeneration: a proinflammatory cytokine inhibits receptor signaling by a survival peptide. *Proc. Natl. Acad. Sci. U. S. A.* 96:9879–84.
47. Shen WH, *et al.* (2004) Tumor necrosis factor alpha inhibits insulin-like growth factor I-induced hematopoietic cell survival and proliferation. *Endocrinology.* 145:3101–5.
48. Sims-Robinson C, Kim B, Rosko A, Feldman EL. (2010) How does diabetes accelerate Alzheimer disease pathology? *Nat. Rev. Neurol.* 6:551–9.
49. Turner JR. (2009) Intestinal mucosal barrier function in health and disease. *Nat. Rev. Immunol.* 9:799–809.
50. Suzuki T, Yoshinaga N, Tanabe S. (2011) Interleukin-6 (IL-6) regulates claudin-2 expression and tight junction permeability in intestinal epithelium. *J. Biol. Chem.* 286:31263–71.
51. Seynhaeve AL, Vermeulen CE, Eggermont AM, ten Hagen TL. (2006) Cytokines and vascular permeability: an in vitro study on human endothelial cells in relation to tumor necrosis factor-alpha-primed peripheral blood mononuclear cells. *Cell. Biochem. Biophys.* 44:157–69.
52. Li L, Elliott JF, Mosmann TR. (1994) IL-10 inhibits cytokine production, vascular leakage, and swelling during T helper 1 cell-induced delayed-type hypersensitivity. *J. Immunol.* 153:3967–78.